

Supporting Information

**Crystalline chlorinated contorted hexabenzocoronene: a
universal organic anode for advanced alkali-ion batteries**

Kijoo Eom,^{‡a} Minsung Kang,^{‡bc} Ju Hyun Park,^{‡a} Se Hun Joo,^a Jaehyun Park,^a Jiseok Lee,^a
Sang Kyu Kwak,^{*a} Seokhoon Ahn,^{*b,d} and Seok Ju Kang^{*a}

^aDepartment of Energy Engineering, School of Energy and Chemical Engineering, Ulsan
National Institute of Science and Technology (UNIST), Ulsan 44919, Republic of Korea

^bInstitute of Advanced Composite Materials, Korea Institute of Science and Technology
(KIST), Jeonbuk 55324, Republic of Korea

^cSchool of Materials Science and Engineering, Gwangju Institute of Science and Technology,
123 Cheomdangwagi-ro, Buk-gu, Gwangju 61005, Republic of Korea

^dDepartment of Chemistry, Jeonbuk National University, 567, Baekje-daero, Deokjin-gu,
Jeonju, Jeollabuk-do 54896, Republic of Korea

Keywords: contorted hexabenzocoronene, organic anode, Li-ion batteries, Na-ion batteries,
and K-ion batteries

Corresponding Author

*E-mail: sjkang@unist.ac.kr, ahn75@kist.re.kr, skkwak@unist.ac.kr

1. Computational details

Crystal structure prediction

To determine the crystal structure of Cl-CHBC, Monte Carlo simulated annealing was performed using the Polymorph module in Materials Studio 2019.¹ Using the optimized molecular structure of Cl-CHBC, several potential crystal structures were generated using the following six sequential steps: packing, clustering, geometry optimization, clustering, geometry optimization, and clustering. In the packing step, numerous crystal structures were sampled by the Monte Carlo simulated annealing method considering 10 different space groups: $P2_1/c$, $P\bar{1}$, $P2_12_12_1$, $C2/c$, $P2_1$, $Pbca$, $Pna2_1$, Cc , $Pbcn$, and $C2$. To find the global minimum structure within a sufficiently large energy landscape, we set the maximum temperature to 1.5×10^5 K, the minimum temperature to 300 K, the maximum number of steps to 5.0×10^5 , the number of steps to accept before cooling to 100, the minimum move factor to 1.0×10^{-50} , and the heating factor to 0.025. In the geometry optimization step, the lattice parameters and atomic coordinates were relaxed under the constraints imposed by crystallographic symmetry. The Cl-CHBC molecules were treated as rigid bodies in the first geometry optimization step and then fully relaxed in the second geometry optimization step. The maximum number of steps was set to 1.0×10^4 , and the convergence criteria were set to 2.0×10^{-5} kcal mol⁻¹ for the maximum energy change, 0.001 kcal mol⁻¹ Å⁻¹ for the maximum force, 0.001 GPa for the maximum stress, and 1.0×10^{-5} Å for the maximum displacement. In the clustering step, many similar structures were grouped into clusters. The lowest energy structure of each cluster was filtered to remove duplicate crystal structures. The criterion to measure crystal similarity was set to 0.11, which was calculated based on a comparison of radial distribution functions with a cutoff distance of 7 Å and 140 bins. After the final clustering step, the space groups of the predicted crystal structures were reanalyzed, and in silico

screening was carried out through XRD comparison. The interatomic interactions were described by the COMPASS II force field² and calculated using the Ewald summation method.³

MC simulations

To identify the adsorption sites for Li ions in the Cl-cHBC crystal phase, Monte Carlo simulated annealing was performed using the Sorption module in Materials Studio 2019.¹ Based on the metropolis algorithm, the Monte Carlo simulated annealing was carried out 3 times independently with a maximum number of loading steps of 1.0×10^5 , a maximum number of production steps of 1.0×10^7 , and 40 annealing cycles. The interatomic interactions were described by the COMPASS II force field³ with Mulliken⁴ charges obtained from DFT calculations.

DFT calculations

DFT calculations were performed using the Cambridge Serial Total Energy Package (CASTEP).⁵ The generalized gradient approximation with the Perdew–Burke–Ernzerhof (GGA-PBE) functional was used.⁶ The interactions between ions and electrons were described by on-the-fly generated norm-conserving pseudopotentials. A plane-wave basis set with a cutoff energy of 870 eV was employed to expand the wave functions. The van der Waals interactions were corrected by Grimme’s method.⁷ The convergence criterion for self-consistent field calculations was set to 5.0×10^{-7} eV atom⁻¹. The lattice parameters and atomic positions were fully relaxed. The convergence criteria for geometry optimization were set to 5.0×10^{-6} eV atom⁻¹ for energy, 0.01 eV Å⁻¹ for force, 0.02 GPa for stress, and 5.0×10^{-4} Å for displacement. The Brillouin zone was integrated using a $1 \times 3 \times 1$ *k*-point grid with the Monkhorst–Pack scheme for all calculations.⁸ The transition state (TS) was found using linear synchronous transit (LST) and quadratic synchronous transit (QST) methods.⁹ For TS search calculation, lattice parameters were set to the lattice parameters of pristine P2₁/*n* crystal

structure The root mean square (RMS) force convergence was set to 0.25 eV Å⁻¹. The formation energy (E_f) of the Cl-cHBC crystal structure with intercalated Li ions was calculated as a function of the Li content, as follows:

$$E_f = E_{Li_n - Cl - cHBC} - E_{Cl - cHBC} - nE_{Li}$$

where $E_{Li_n - Cl - cHBC}$ is the total energy of the Cl-cHBC crystal with intercalated Li ions, n is the number of intercalated Li ions, $E_{Cl - cHBC}$ is the total energy of the P2₁/n crystal phase of Cl-cHBC, and E_{Li} is the total energy per atom of bcc bulk Li. The voltage profile as a function of intercalated Li ions was calculated as follows:

$$V(n) = - \frac{E_{Li_{n_2} - Cl - cHBC} - E_{Li_{n_1} - Cl - cHBC} - (n_2 - n_1)E_{Li}}{q(n_2 - n_1)}$$

where $E_{Li_{n_1} - Cl - cHBC}$ and $E_{Li_{n_2} - Cl - cHBC}$ represent the total energies of Cl-cHBC crystals with intercalated Li ions, n_1 and n_2 are the numbers of intercalated Li ions ($n_2 > n_1$), and q is the net charge of a Li ion ($q = +1e$).

DFT calculations for two stacked Cl-cHBC molecules with an intercalated metal ion

To investigate the molecular stacking structures of Cl-cHBC molecules, spin-polarized DFT calculations were conducted using the DMol3 module¹⁰ in Materials Studio 2019.¹ The GGA-PBE functional was employed to describe the exchange-correlation potential of electrons.⁶ The DNP 4.4 basis set was used with a global orbital cutoff of 3.7 Å. The core electrons were explicitly treated as all electrons with a relativistic effect. The long-range van der Waals interactions were corrected using Grimme's method.⁷ The self-consistent field calculation was performed with a fixed orbital occupancy, until the convergence criterion of 1.0×10^{-6} was satisfied. The convergence criteria for geometry optimization were set to 1.0×10^{-5} Ha for the

maximum energy change, $0.002 \text{ Ha } \text{\AA}^{-1}$ for the maximum force, and 0.005 \AA for the maximum displacement. The deformation energy (E_{def}) of the stacked Cl-cHBC molecules was calculated as follows:

$$E_{\text{def}} = E_{\text{def-cl-cHBCmol}} - E_{\text{Cl-cHBCmol}}$$

where $E_{\text{def-cl-cHBCmol}}$ is the total energy of the stacked Cl-cHBC molecules (i.e., without a metal ion) after the intercalation of a metal ion, and $E_{\text{Cl-cHBCmol}}$ is the total energy of the stacked Cl-cHBC molecules before the intercalation of a metal ion.

2. Supporting figures

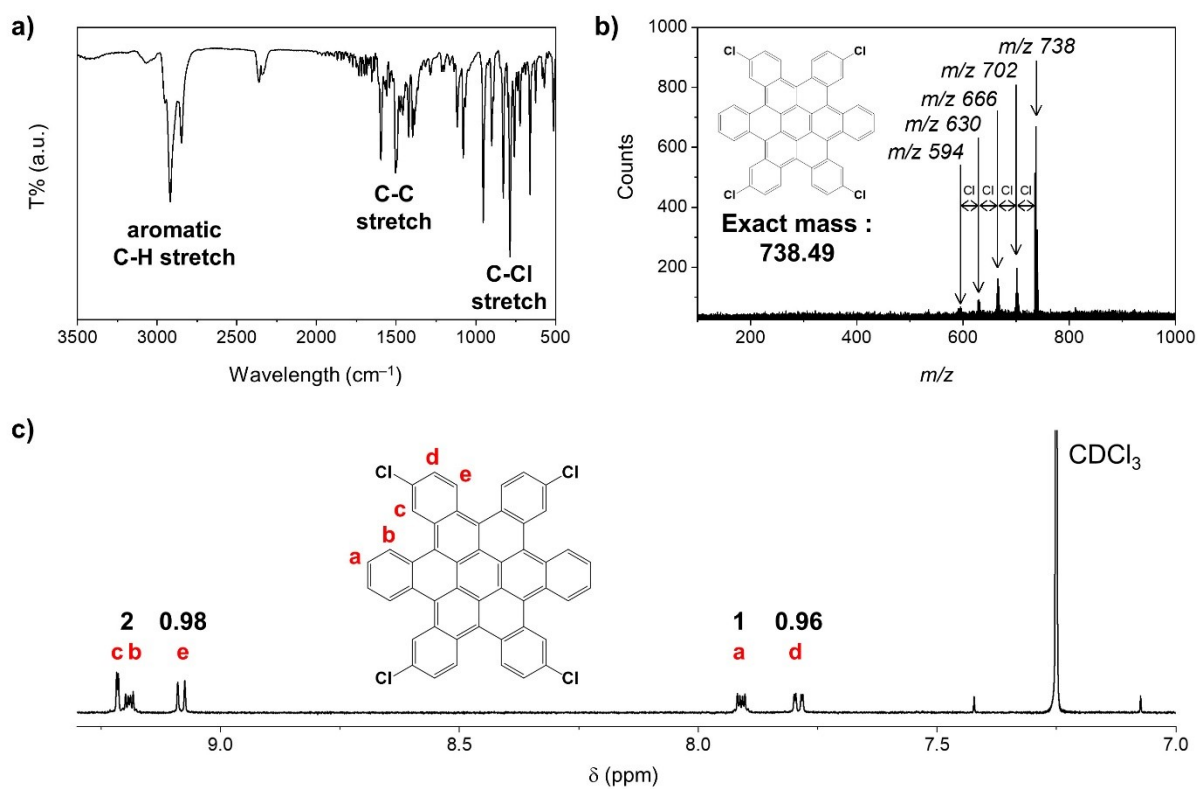


Fig. S1. (a) IR, (b) mass, and (c) NMR characteristics of Cl-cHBC molecule

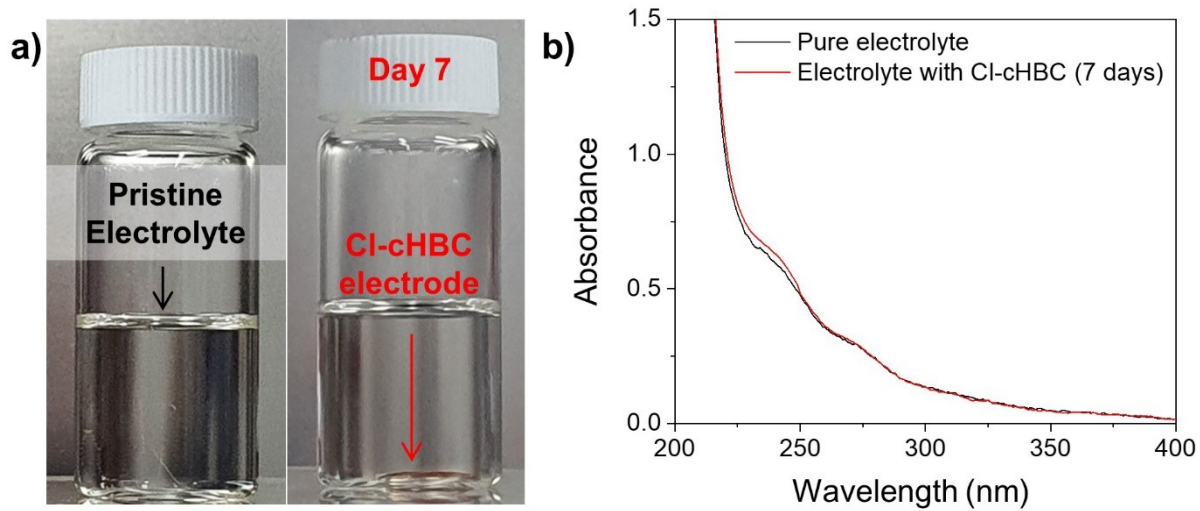


Fig. S2. (a) Digital photographs and (b) UV-vis spectra of the pristine electrolyte (black line) and electrolyte after immersing the Cl-cHBC electrode for 7 days

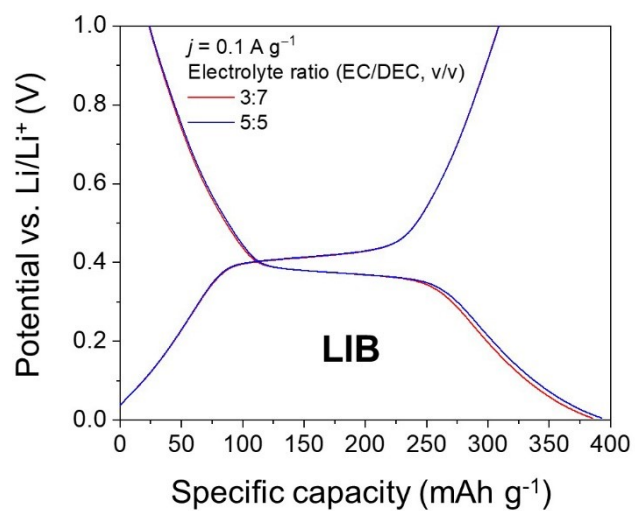


Fig. S3. Galvanostatic discharge/charge plots of Cl-cHBC anode for LIB at a current density of 0.1 A g^{-1} containing 1.3 M LiPF_6 in EC:DEC, 3:7 (red) and 5:5 (blue line) + FEC 10 wt% electrolytes

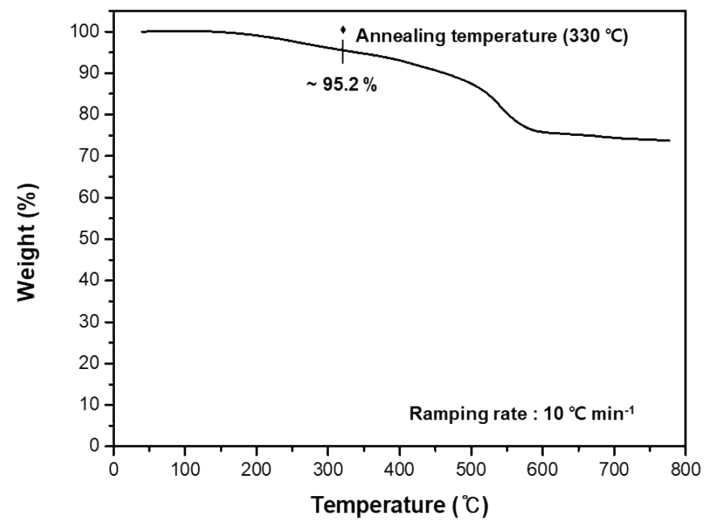


Fig. S4. TGA thermogram of pristine Cl-cHBC powder

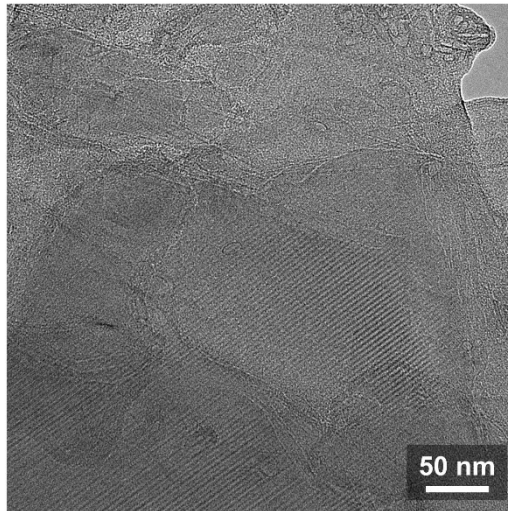


Fig. S5. Cross-sectional HRTEM image of 330 °C annealed Cl-cHBC anode

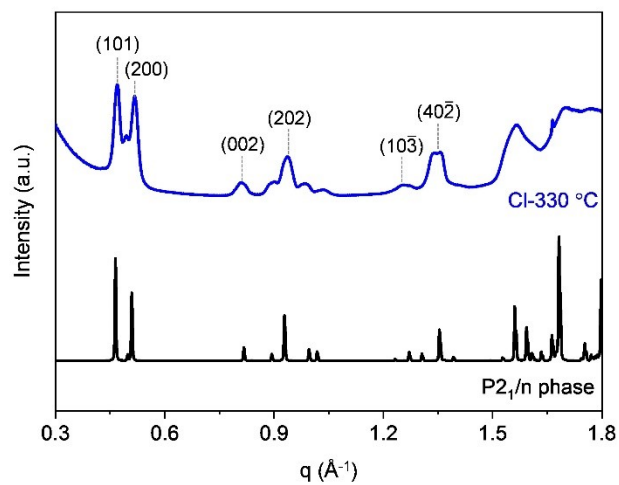


Fig. S6. XRD patterns of Cl-cHBC: experimental pattern (blue line) and simulated pattern of the $P2_1/n$ crystal structure optimized using DFT calculation (black line). The lattice parameters of the optimized crystal structure were $a = 24.76 \text{ \AA}$, $b = 4.08 \text{ \AA}$, $c = 15.43 \text{ \AA}$, $\alpha = 90.00^\circ$, $\beta = 85.53^\circ$, and $\gamma = 90.00^\circ$.

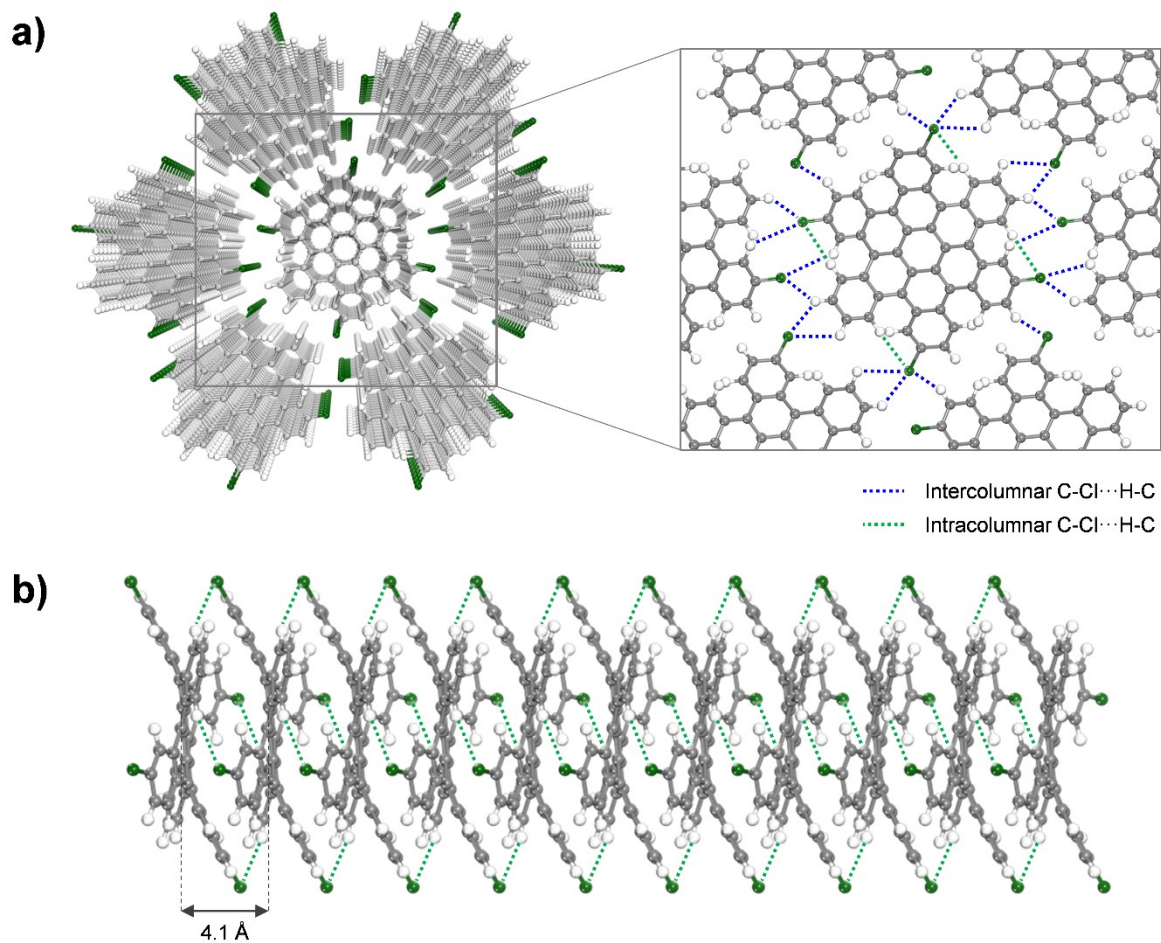


Fig. S7. Structure of Cl-chBC crystallized in the monoclinic $P2_1/n$ space group. (a) Top view of molecular columns arranged in a distorted hexagonal manner. (b) Side view of a molecular column. The blue and green dashed lines represent intercolumnar C-Cl...H-C interactions between the central and adjacent molecular columns and intracolumnar C-Cl...H-C interactions in the central molecular column, respectively. Carbon, hydrogen, and chlorine atoms are represented in gray, white, and green, respectively.

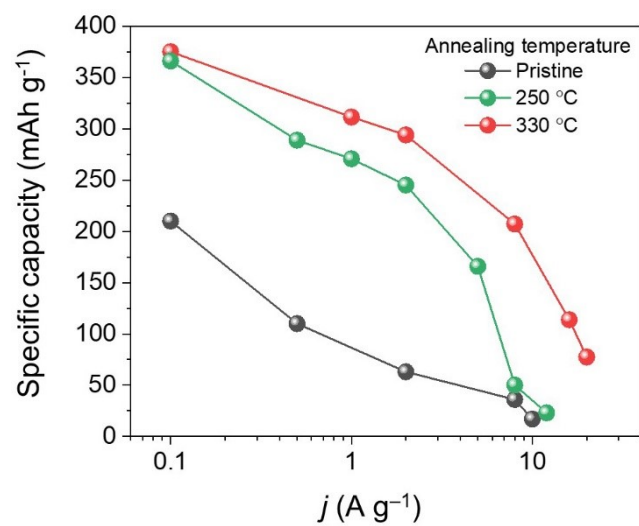


Fig. S8. Plots of specific capacity versus current density for pristine, 250 °C and 330 °C annealed Cl-cHBC anodes

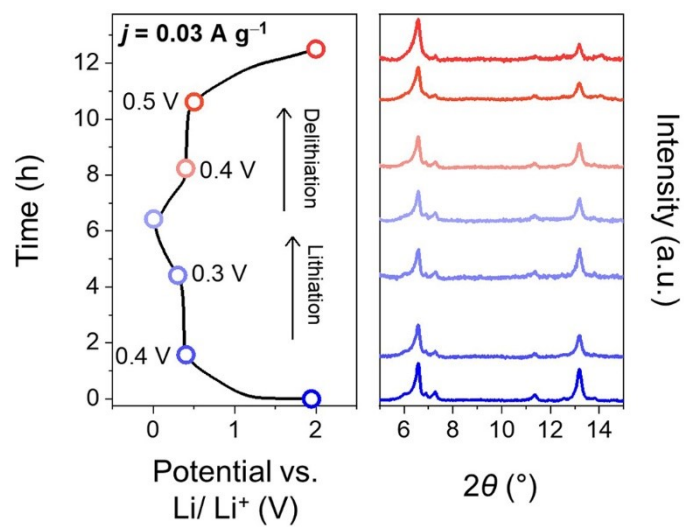


Fig. S9. *Ex-situ* XRD patterns of Cl-CHBC electrodes consecutively collected during the lithiation and de-lithiation processes.

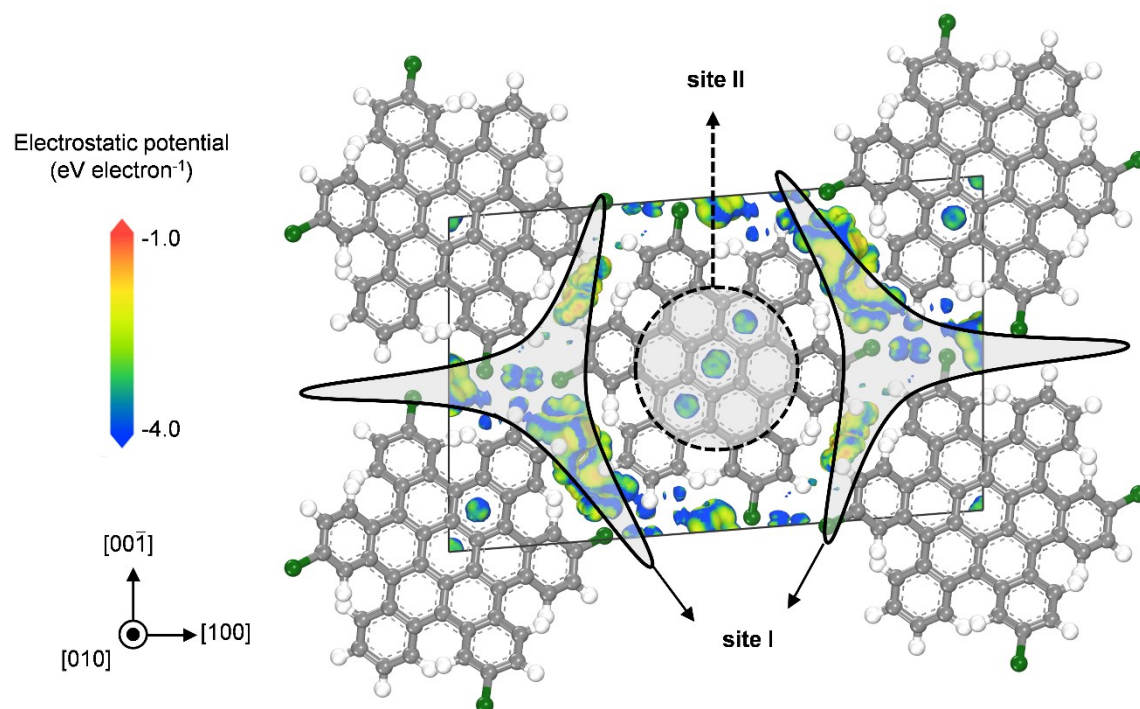


Fig. S10. Projection view of the optimized $P2_1/n$ crystal structure of Cl-cHBC with a Connolly surface. Electrostatic potentials are mapped onto the Connolly surface. Sites I and II represent the space between the molecular columns and the space between the stacked molecules within a column, respectively. Carbon, hydrogen, and chlorine atoms are represented in gray, white, and green, respectively.

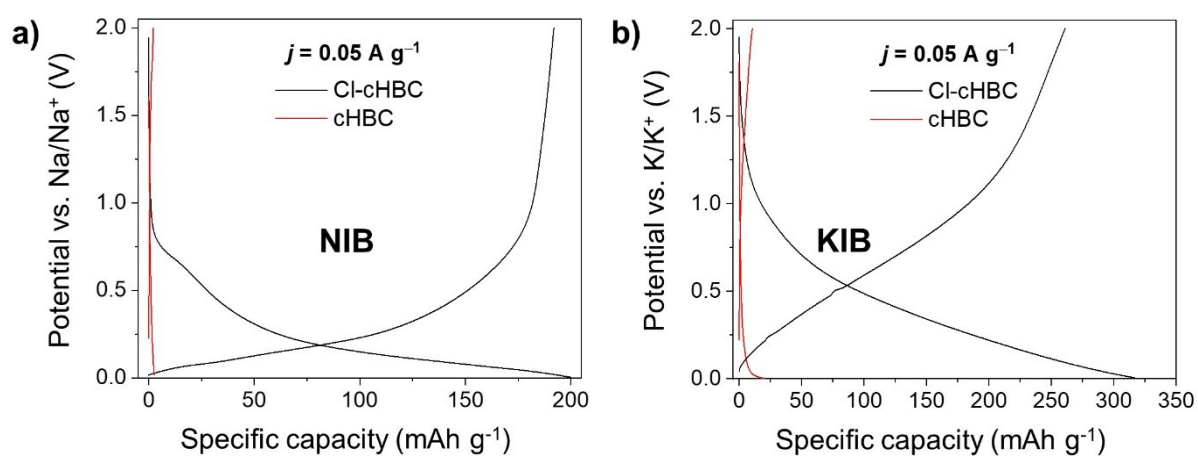


Fig. S11. Galvanostatic discharge/charge plots of Cl-cHBC and cHBC anodes for (a) NIB and (b) KIB

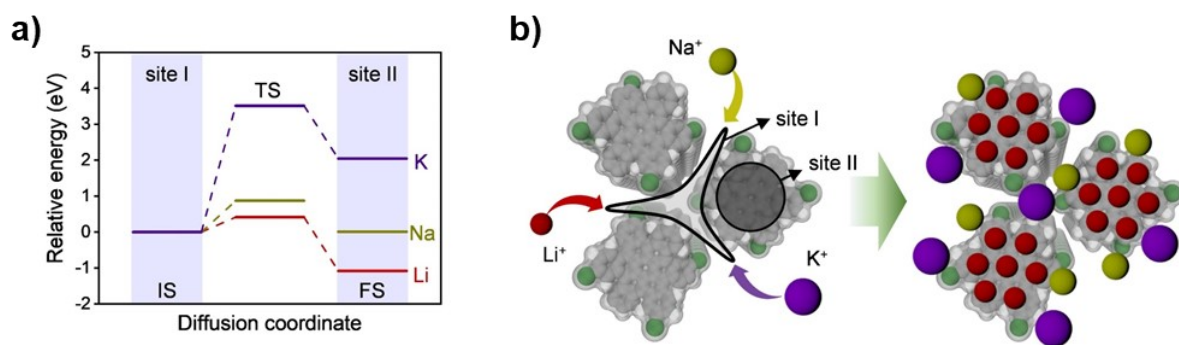


Fig. S12. (a) Comparison of activation energies required for the intercalation of Li, Na, and K ions into site II from site I. IS, TS, and FS represent the initial state of the metal ion adsorbed at site I, the transition state, and the final state of the metal ion intercalated into site II, respectively. (b) Schematic representation of the different intercalation behaviors of Li, Na, and K ions. Carbon, hydrogen, chlorine, lithium, sodium, and potassium atoms are represented in gray, white, green, red, dark yellow, and purple, respectively.

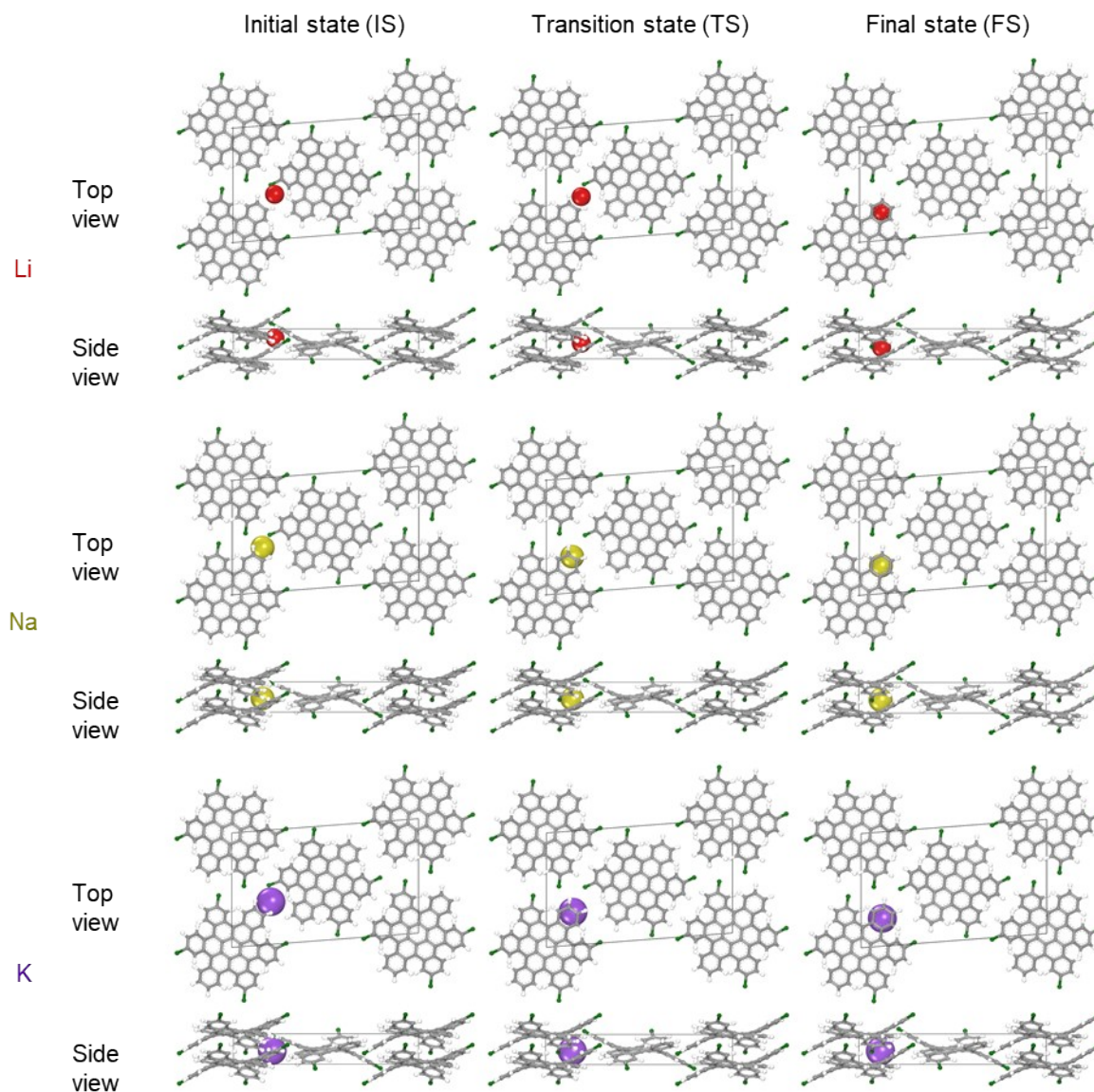


Fig. S13. Initial state, transition state, and final state configurations for the intercalation of Li, Na, and K ions into site II from site I. Carbon, hydrogen, chlorine, lithium, sodium, and potassium atoms are represented in gray, white, green, red, dark yellow, and purple, respectively.

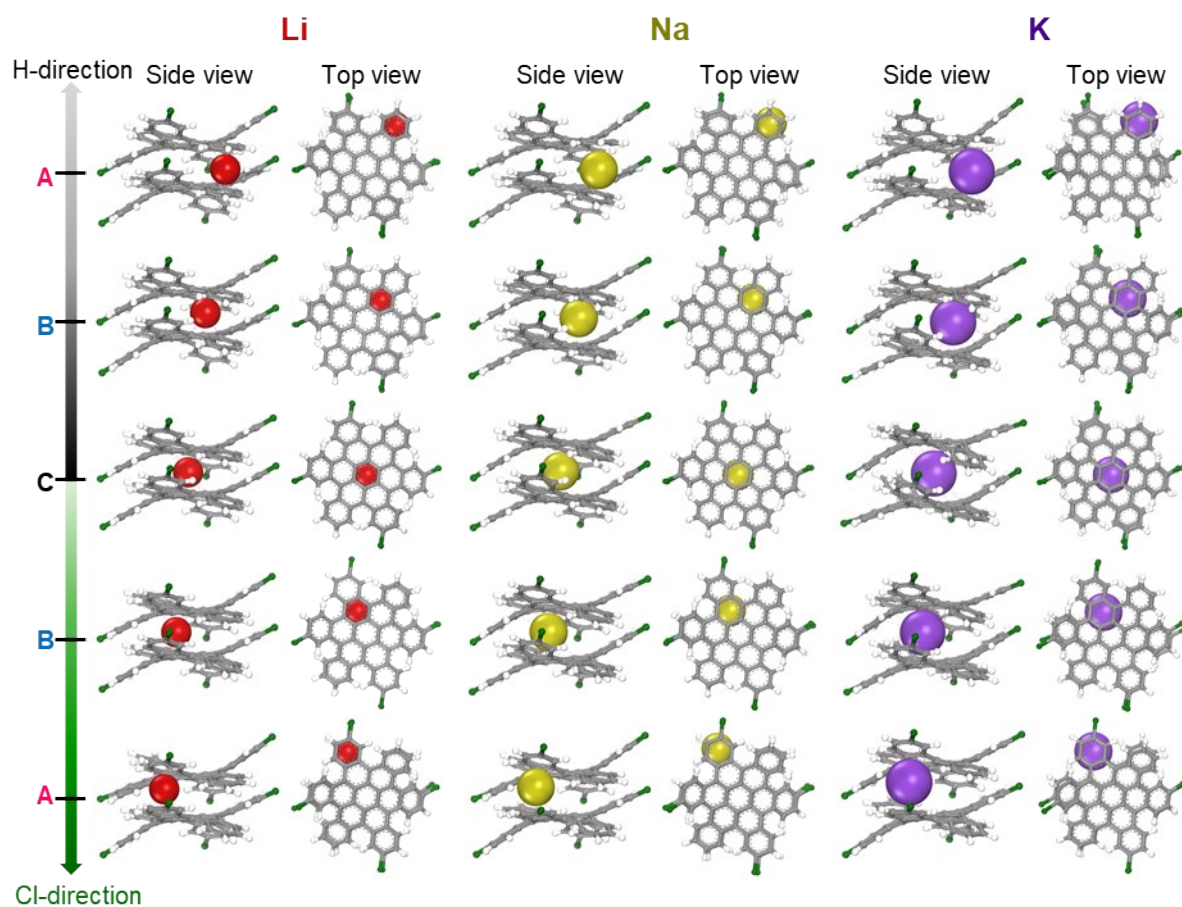


Fig. S14. Optimized structures of stacked Cl-cHBC molecules with different intercalated metal ions. Carbon, hydrogen, chlorine, lithium, sodium, and potassium atoms are represented in gray, white, green, red, dark yellow, and purple, respectively.

Supporting Information References

1. Dassault Systèmes BIOVIA, Materials Studio, 2019 San Diego: Dassault Systèmes 2019
2. H. Sun, Z. Jin, C. Yang, R. L. C. Akkermans, S. H. Robertson, L. A. Spenley, S. Miller, S. M. Todd, *J. Mol. Model.*, 2016, **22**, 1–10.
3. P. P. Ewald, *Annalen der Physik*, 1921, **369**, 253–287.
4. R. S. Mulliken, *J. Chem. Phys.*, 1955, **23**, 1833–1840.
5. S. J. Clark, M. D. Segall, C. J. Pickard, P. J. Hasnip, M. I. J. Probert, K. Refson, M. C. Payne, *Zeitschrift für kristallographie-crystalline materials*, 2005, **220**, 567–570.
6. J. P. Perdew, K. Burke, M. Ernzerhof, *Phys. Rev. Lett.*, 1996, **77**, 3865–3868.
7. S. Grimme, *J. Comput. Chem.*, 2006, **27**, 1787–1799.
8. H. J. Monkhorst, J. D. Pack, *Phys. Rev. B*, 1976, **13**, 5188–5192.
9. S. Bell, J. S. Crighton, *J. Comput. Chem.*, 1984, **80**, 2464–2475.
10. T. A. Halgren, W. N. Lipscomb, *Chem. Phys. Lett.*, 1977, **49**, 225–232.
11. B. Delley, *J. Chem. Phys.*, 1990, **92**, 508–517.
12. B. Delley, *J. Chem. Phys.*, 2000, **113**, 7756–7764.